Research Journal of Applied Sciences, Engineering and Technology 4(1): 59-65, 2012
ISSN: 2040-7467

Submitted: September 14, 2011 Accepted: October 15, 2011 Published: January 01, 2012

Fractional Fourier Transform Based Pilot Symbol Assisted Modulation

[1]Simranjit Singh, [1]Rajesh Khanna and [2]Manjeet Patterh
[1]Electronics and Communication Eng ineering Department, Thapar University, Punjab, India
[2]University College of Engineering, Punjabi University, Patiala, Punjab, India

Abstract: In this study, a novel Fractional Fourier transform (FrFT) based pilot symbol assisted modulation (FPSAM) technique for channel estimation has been proposed. In FPSAM, the received pilot symbols are processed in fractional Fourier domain before being used for channel estimation. In practice, the channel estimation is done by sending known training (pilot) symbols along with the information symbols and the quality of Channel State Information (CSI) obtained from the pilot symbols depends on the technique used for channel estimation. The proposed method helps in obtaining accurate channel estimates due to effective removal of noise in the optimum fractional domain. For spline interpolation, FPSAM gives an SNR improvement of 1.90 dB as compared to conventional PSAM for a BER of 10^{-2}. It is shown through simulations that the proposed method clearly outperforms the existing method.

Key words: CSI, interpolation, PSAM, 16-QAM

INTRODUCTION

With the rapid growth of digital communication in recent years, the need for high speed data transmission has increased. The use of multilevel modulation schemes such as 16-QAM and 64-QAM having high spectral efficiency is desirable. For achieving high spectral efficiency reliably, the Channel State Information (CSI) should be known to the receiver. The channel response can be obtained at the receiver by using Pilot Symbol Assisted Modulation (PSAM), in which the transmitter periodically inserts pilots (known symbols), into the information stream (Cavers, 1991; Torrance and Hanzo, 1995). These pilot symbols can be recovered and used at the receiver to obtain an estimate of the amplitude and phase of the channel response. Knowing the CSI also makes it possible to adapt transmissions to current channel conditions. The CSI describes how a signal propagates from the transmitter to the receiver and represents the combined effect of, for example, scattering, fading, and power decay with distance. The severe amplitude and phase fluctuations inherent to wireless channels inhibits the use of high level QAM schemes because the demodulator has to scale the received signal to normalize the channel gain so that its decision regions correspond to the transmitted signal constellation. This process is called Automatic Gain Control (AGC) (Webb and Hanzo, 1994). If the channel is estimated poorly, the amplitude and phase reference obtained is improper and the Bit Error Rate (BER) is very high. Thus, the use of an accurate channel estimation technique enables the efficient use of the multilevel QAM modulation schemes (Sampei and Sunaga, 1993). The channel may have changed from the pilot symbol time instant to the data symbol time instant, therefore, the channel gain at the data symbol is estimated using multiple pilot symbols and an interpolation filter. The interpolation filter helps to construct the channel response at data points with the help of discrete set of known channel response at the pilot points. The estimates obtained by interpolation are valid because of the time correlation of the fading channel. The channel estimates can also be obtained using blind estimation or decision directed techniques but their performance is inferior to PSAM (Proakis, 2001). In practice, the channel estimation is never perfect and noise errors are always present in the estimated channel response. These errors can be reduced by estimating the pilot symbols using Fractional Fourier Transform (FrFT). In this study, we propose a novel FrFT based PSAM (FPSAM) technique for obtaining better estimates of pilot symbols.

MATERIALS AND METHODS

Pilot Symbol Assisted Modulation (PSAM): The block diagram of a conventional PSAM system is shown in Fig. 1. The symbols are transmitted in frames of length *N*. Without loss of generality, assume that, in each frame, the first symbol is a pilot symbol b(0) , and the remaining N-1 symbols are the data symbols b(1), b(2), …, b(N-1). The data symbols are modulated by Gray coded 16-QAM;

Corresponding Author: Simranjit Singh, Electronics and Communication Engineering Department, Thapar University,Punjab, India

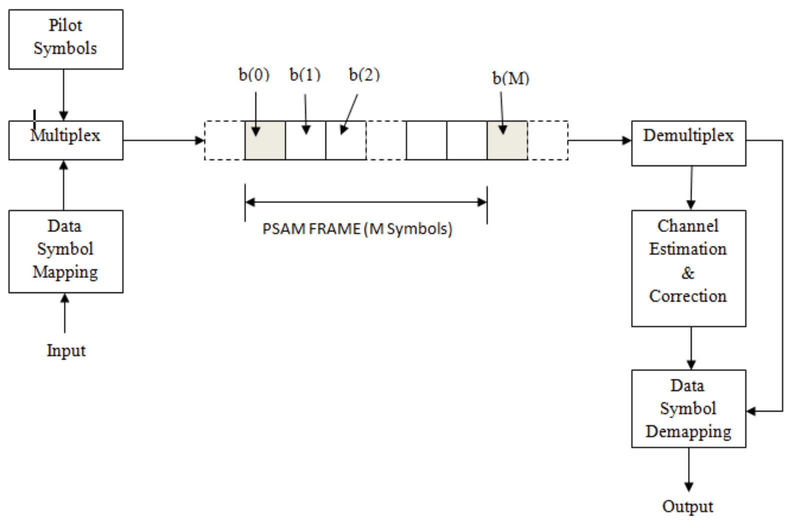

Fig. 1: Schematic of conventional PSAM System showing the frame structure (Torrance and Hanzo, 1995)

therefore, the data symbol belongs to the set of 16 possible signals. The pilot symbols have a fixed value b which is known to the receiver. The transmitted signal has a complex envelope given by:

$$s(t) = \sum_{k=-\infty}^{\infty} b(k)\, p(t - kT) \tag{1}$$

where, T is the symbol duration, b(k) represents the In-phase or Quadrature components of the symbols to be transmitted and p(t) is a band limited unit energy signaling pulse, for which we have:

$$\int_{-\infty}^{\infty} |p(t)|^2 \, dt = 1 \tag{2}$$

The received signal for a narrowband Rayleigh channel is given by:

$$r(t) = c(t).s(t) + n(t) \tag{3}$$

where, n(t) is AWGN with variance $\sigma^2_n = N_0/2$ and c(t) is the complex channel gain:

$$c(t) = \alpha(t) e^{j\theta(t)} \tag{4}$$

where, α(t) is the Rayleigh fading envelope and θ(t) is the uniformly distributed phase. The output of the matched filter at sampling instant kT is given by:

$$r(k) = c(k).b(k) + n(k) \tag{5}$$

The pilot symbols are inserted at times i = Kn, therefore, the pilot symbols are represented by r(iN) and the estimated channel response ĉ(iN) at the pilot positions is calculated by:

$$\hat{c}(iN) = r(iN) / \tilde{b} \tag{6}$$

$$\hat{c}(iN) = c(iN) + \frac{n(iN)}{\tilde{b}} \tag{7}$$

$$\hat{c}(iN) = \hat{a}(iN) e^{j\hat{\theta}(iN)} \tag{8}$$

where, $\hat{\alpha}$ (iN) is the estimated fading channel envelope and $\hat{\theta}$ (iN) is the estimated phase. From the above expression, it is clear that the channel estimate at pilot positions is affected by noise errors i.e., $n(iN)/\tilde{b}$. The channel response at the data symbol positions is obtained by interpolating the sequence ĉ(iN). The channel state estimator prepares an estimate of ĉ(k) using the K nearest pilot symbols:

$$\hat{c}(k) = \sum_{t=-[K/2]}^{[K/2]} h^*(i,k)\hat{c}(iN) \tag{9}$$

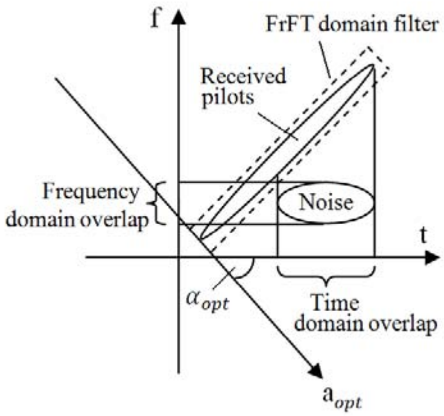

Fig. 2: Filtering in fractional Fourier domain

where, h(i,k) are the interpolation coefficients which explicitly depend on position k within the frame. The estimation error e(k) is given by:

$$e(k) = c(k) - \hat{c}(k) \tag{10}$$

From Eq. (9) we can see that the accurate estimation of ĉ(k) depends on the quality of ĉ(iN). The noise component in Eq. (7) contributes a large percentage of the estimation error especially at low SNR. Hence, any reasonable system that can improve ĉ(iN) and reduce e(k) will improve c(k). One such system is the FrFT based PSAM (FPSAM) in which the received pilot symbols r(iN) are processed in the fractional Fourier domain before channel estimation is performed. By processing r(iN) in the fractional domain, the effect of noise on the pilot symbols is minimized and therefore the estimation error e(k) is reduced. The motivation behind the proposed method is the ability of FrFT to reduce the effect of noise on the received symbols. A detailed description of FPSAM is given in the following section.

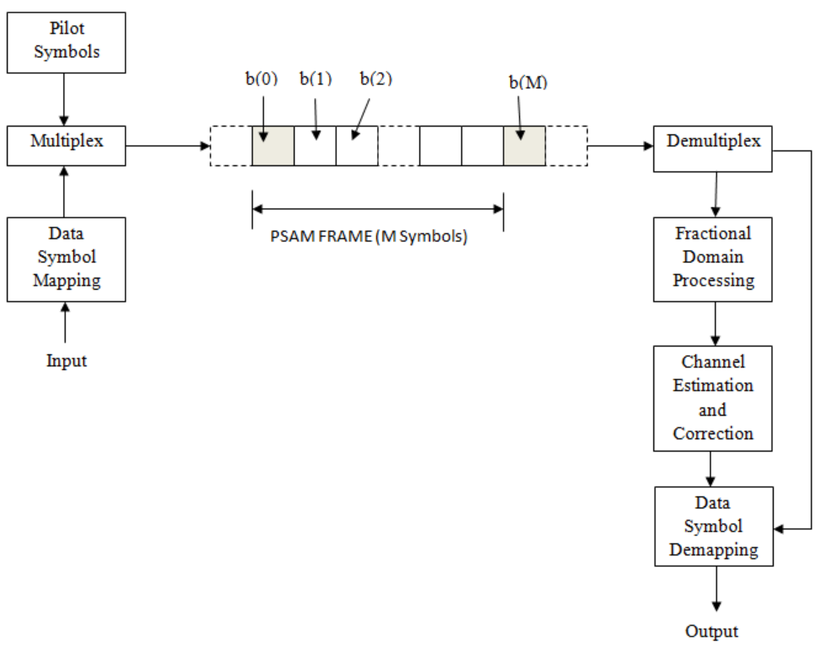

Fig. 3: Schematic of FPSAM system showing the frame structure

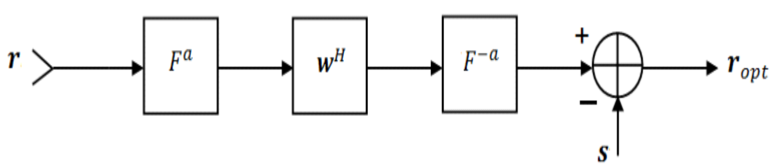

Fig. 4: Internal diagram of fractional domain processing block

Fractional Fourier transform based PSAM (FPSAM): The continuum of fractional Fourier domains corresponds to the oblique axes in time frequency plane, with ordinary time and frequency domains as special cases as shown in Fig. 2. The FrFT is a linear transformation generalizing the Fourier Transform (FT). In classical Fourier transform the signal is rotated by $\pi/2$ in the time-frequency plane. So, FrFT can be thought of as FT to the a^{th} power, where 'a' needs not be an integer - thus, it can transform a function to an intermediate domain between time and frequency. The fractional domain for a = 0 corresponds to time domain and a = 1 corresponds to frequency domain. The received pilot symbols r(iN) appear to be non compact and scattered in time and frequency due to the effect of multiplicative fading and additive noise in the wireless channel (Fig. 2). The FrFT can be thought of as a time varying filter which provides an order 'a' or 'a' on the time-frequency plane where the non compact pilot symbol appears to be compact and best estimated. From Fig. 2, it is clear that the pilot symbols can be best estimated in 'a^{th}' domain because in the conventional time and frequency domains, the received pilot symbols are overlapping with the noise. For a detailed description of FrFT and its application to wireless communication, refer to Khanna and Saxena (2009, 2010), Ozaktas *et al*. (1994, 2000), Yetik *et al.* (2000) and Yetik and Nehorai (2003).

Define the length K column vectors r and s as the set of received pilot samples r (iN) and transmitted pilot samples s (iN) . Also, define the length K column vector c as the set of channel coefficients at pilot positions. Figure 3 shows the block diagram of FPSAM and Fig. 4 shows the internal diagram of the fractional domain processing block.

The transmitted and received pilot symbol vectors s and r are transformed from time domain to the fractional Fourier domain by using the transformation kernel K_a or K_a (Ozaktas *et al.*, 2000):

$$r_a = F^a\{r\}\ ,\ s_a = F^a\{s\} \tag{11}$$

where, F^a denotes the a^{th} order FrFT. After r_a is obtained, the filtering process is performed using the Wiener filtering technique (Kutay *et al.*, 1997; Tse and Viswanath, 2005). The optimal Wiener solution in the fractional domain is given by:

$$w_a = R^{-1}_{r_a r_a} R_{r_a s_a} \tag{12}$$

where, w_a is the weight vector in the a^{th} domain, $R_{ra\,ra}$ is the auto covariance of the vector r in the ath domain and $R_{ra\,ra}$ is the cross covariance of r and s in the a^{th} domain. $R_{ra\,ra}$ and $R_{ra\,sa}$ are given by:

$$R_{r_a s_a} = F^a(R_{ss}H^H)F^{-a} \tag{13}$$

$$R_{r_a r_a} = F^a(HR_{ss}H^H + R_{nn})F^{-a} \tag{14}$$

where, F^{-a} denotes the inverse a^{th} order FrFT. The Wiener solution given in Eq. (12) reduces to time domain wiener solution for a = 0 and frequency domain wiener solution for a = 1. The optimum value of 'a' is simply found by calculating the Mean Squared Error (MSE) for sufficiently closely spaced discrete values of 'a' $\epsilon[-1,1]$ and choosing the one which minimizes the MSE. The MSE is calculated by:

$$MSE(w_a) = E\{\|s - F^{-a}w_a^H F^a r\|^2\} \tag{15}$$

where, E{*} denotes the expectation operator and ||*|| is the L_2 norm. The key point is that for a given the noise and signal statistics, the value of optimum order 'a_{opt}' is calculated only once. After this, the estimation process can be implemented in time for arbitrary many realizations of that given statistics. The optimum order 'a_{opt}' is only recalculated again when the noise and signal statistics change. After the optimum order is calculated, the weight vector is calculated in the optimum domain using Eq. (12). The weight vector calculated in the optimum domain (a_{opt}) is called optimum weight vector (w_{opt}).

$$w_{opt} = R^{-1}_{r_a r_a} R_{r_a s_a} \tag{16}$$

After Wiener filtering in the optimum domain, the signal is converted back to its original domain by using inverse FrFT. After optimum domain filtering, the effect of AWGN on r is minimized, therefore, it is denoted by r_{opt}:

$$r_{opt} = F^{-a}\{w_{opt}^H(F^a\{r\})\} \tag{17}$$

The MSE given by Eq. (15) is minimum for $w_a = w_{opt}$. As discussed above, the value of 'a' which minimizes the MSE is chosen to be optimum. Also, the accuracy of 'a_{opt}' depends on the step size of the discrete values of 'a', e.g., in this study the step size is taken to be 0.1. After r_{opt} is obtained, the CSI at the pilot positions can be calculated for r_{opt} using Eq. (6):

$$\hat{c}_{opt}(iN) = \frac{r_{opt}(iN)}{\tilde{b}} \quad (18)$$

where, $\hat{c}_{opt}(iN)$ is the optimum CSI at pilot positions. In terms of optimum estimated envelope $(\hat{\alpha}_{opt})$ and phase ($\hat{\theta}_{opt}$), $\hat{c}_{opt}(iN)$ is given by:

$$\hat{c}_{opt}(iN) = \hat{\alpha}_{opt}(iN)e^{j\hat{\theta}_{opt}(iN)} \quad (19)$$

Channel interpolation: After the estimation of the channel response at the pilot positions, the channel response at data positions can be obtained by interpolating $\hat{c}_{opt}(iN)$ using Eq. (9):

$$\hat{c}_{opt}(k) = \sum_{i=-[K/2]}^{[K/2]} h^*(i,k)\hat{c}_{opt}(iN) \quad (20)$$

where, $\hat{c}_{opt}(iN)$ is the optimum estimated channel with estimated envelope $\hat{\alpha}_{opt}$ and phase $\hat{\theta}_{opt}$. In terms of $\hat{\alpha}_{opt}$ and $\hat{\theta}_{opt}$, $\hat{c}_{opt}(iN)$ is given by:

$$\hat{c}_{opt}(k) = \hat{\alpha}_{opt}(k)e^{j\hat{\theta}_{opt}(k)} \quad (21)$$

In Eq. (19) the term h*(i,k) denotes the interpolation coefficients. These coefficients explicitly depend on the position of k within the frame. The interpolation techniques which have been used in this study to obtain h*(i,k) are listed below:

- Linear Interpolation
- Spline Interpolation
- FFT interpolation

Computational complexity of FRFT: For time-invariant degradation models and stationary signals and noise, the classical Fourier domain Wiener filter can be implemented in O (L $\log_2$ L) time, where *L* is the temporal length of the signal. However, for time varying degradations and non stationary processes, the optimal linear estimate requires O (L^2) time for implementation. The filtering process in fractional Fourier domain, which enables significant improvement of the received pilot symbols, can be implemented in O (L $\log_2$ L) time. Thus, improved performance is achieved at no additional cost (Ozaktas *et al.*, 1994, 1996; Yetik *et al.*, 2000).

Simulation details: The number of information bits is 1593. The frame length (*N*) is 10 and the first symbol in each frame is a known pilot symbol. The number of pilot

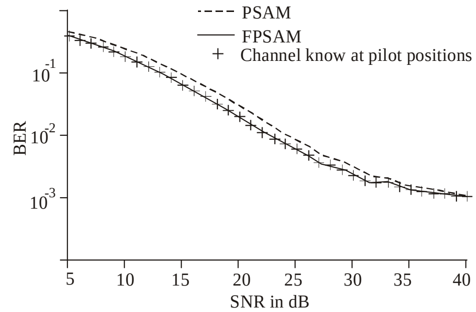

Fig. 5: BER vs. SNR for PSAM and FPSAM using FFT interpolation

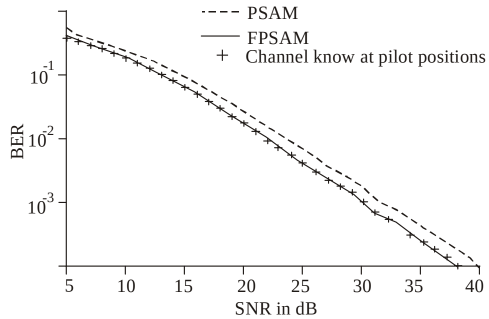

Fig. 6: BER vs. SNR for PSAM and FPSAM using spline interpolation

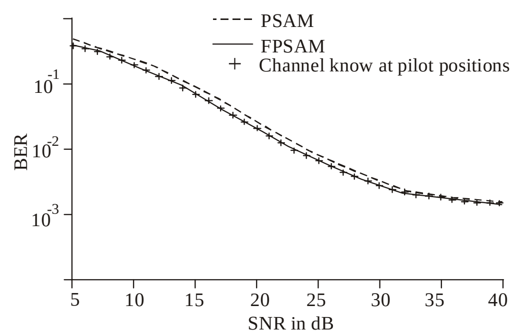

Fig. 7: BER vs. SNR for PSAM and FPSAM using spline interpolation

symbols is 177 and the total number of transmitted symbols (data symbols + pilot symbols) is 1770. The modulation scheme used is Gray-coded 16-QAM. The channel is considered to be flat Rayleigh faded and noise is modeled as additive white Gaussian noise (AWGN). Both the fading channel and noise are comprised of i.i.d complex Gaussian random variables CN(0,1). The value of FrFT order ‘a’ is varied from -1 to +1 with a step size of 0.1. A total of 21 values of ‘a’ are investigated, selecting the one which gives the minimum MSE. For finding the BER, the SNR is varied from 0 to 40 dB in a step of 1dB with 500 iterations done on each value of

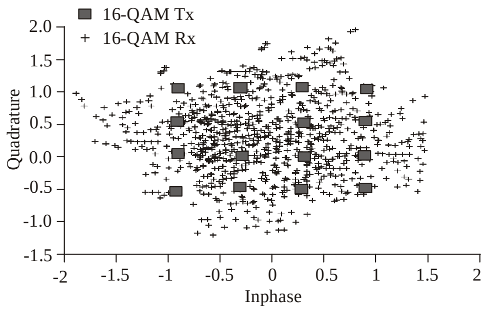

Fig. 8: Comparison of transmitted 16-QAM signal with received 16-QAM signal (before demodulation) distorted by noise and fading

Table 1: BER improvement of FPSAM over PSAM for a fixed SNR of 10 dB

(SNR = 10dB)	Linear (BER)	FFT (BER)	Spline (BER)
CPSAM	0.1571	0.1682	0.1642
FPSAM a = (0.3)	0.1330	0.1322	0.1312

Table 2: BER improvement of FPSAM over PSAM for a fixed SNR of 15 dB

(SNR = 15dB)	Linear (BER)	FFT (BER)	Spline (BER)
CPSAM	0.0726	0.0796	0.0764
FPSAM a = (-0.2)	0.0587	0.0581	0.0566

Table 3: SNR improvement of FPSAM over PSAM for a fixed BER of 10^{-2}

(BER = 10^{-2})	Linear (SNR)	FFT (SNR)	Spline (SNR)
CPSAM	25.49	25.73	24.79
FPSAM	24.32	23.99	22.89

SNR to give statistically justified results. Three interpolation techniques, namely, linear, spline and FFT interpolation have been used for simulations. All the simulations have been done using MATLAB. This study was conducted in Thapar University, India in the year 2011.

RESULTS AND DISCUSSION

In this study, a method to improve channel estimation by filtering the received pilot symbols in fractional Fourier domains has been presented. In conventional PSAM, the received pilots are used for channel estimation without any kind of processing, which results in inaccurate channel estimation. Fig. 5 shows the BER vs. SNR performance of PSAM and FPSAM for spline interpolation technique. It is seen that the proposed method gives lower BER at all SNRs as compared to PSAM. Fig. 6 and 7 show similar results for FFT and linear interpolation techniques respectively. The results shown in Fig. 6, 7 and 8 are summarized in Table 1, 2 and 3. Table 1 and 2 compare the BER of two techniques for fixed SNRs of 10 and 15 dB. It is seen that as compared to PSAM, lower BER can be achieved by using

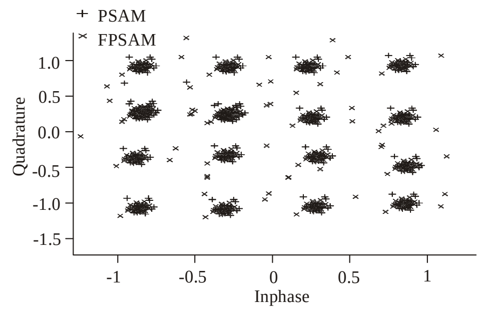

Fig. 9: Demodulated 16-QAM for PSAM and FPSAM using linear interpolation

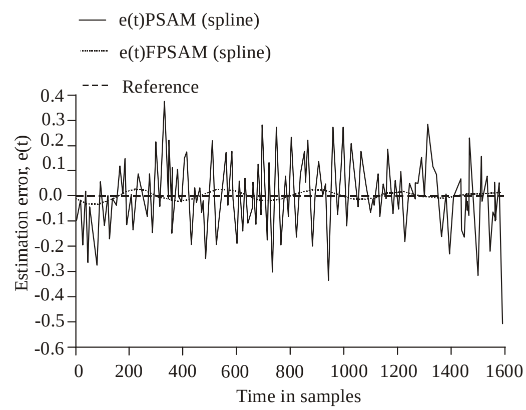

Fig. 10: Estimation error e (t) for PSAM and FPSAM using spline interpolation at a fixed SNR of 10 dB

FPSAM for same SNR. Also, Table 3 compares the SNR for a fixed BER of 10^{-2} and it is shown that the proposed technique gives an SNR advantage in all the three cases. Also, from Fig. 5, 6 and 7, it can be observed that the error performance of FPSAM is very close to the ideal case when the exact channel response at pilot positions is known.

The effect of AWGN and fading on the transmitted signal is shown in Fig. 8. The signal appears to be completely scattered and the information carried by it is unintelligible in this form. To demodulate this signal properly, accurate channel estimates at the data positions are required. These estimates are obtained by interpolating the channel response at pilot positions. The quality of the demodulation depends on the accuracy of the channel estimation. Figure 9 compares the PSAM demodulated signal with the FPSAM demodulated signal. The results in Fig. 9 are obtained for linear interpolation at a fixed SNR of 30 dB. The signal demodulated using the estimates obtained by FPSAM appears to be compact whereas the signal obtained by using channel estimates obtained for PSAM appears to be scattered. The quality of channel estimates at data positionsobtainedbyinterpolation can be determined by interpolation/estimation error given by Eq. (10). The estimation error using spline interpolation for a fixed SNR of 10 dB is plotted in Fig. 10. From the above results it can be concluded that the performance of FPSAM is better than conventional PSAM.

CONCLUSION

In this study, a fractional Fourier transform based PSAM technique is proposed for channel estimation. The proposed method gives better channel estimates as compared to the conventional PSAM technique. In FPSAM, the received pilot symbols are processed in the fractional Fourier domain before channel response is extracted from them. The fractional domain filtering effectively removes the noise in the received pilot signals, therefore giving a better channel gain estimate at the pilot positions. Accurate estimate of the channel response at pilot symbol positions helps in obtaining accurate channel response at data positions which enables the use of multilevel modulation formats such as 16-QAM and 64-QAM. Moreover, this performance improvement comes at no additional cost since the fractional Fourier transform has an O (N $\log_2$ N) algorithm for time invariant degradation models which is the same as classical Fourier transform. Also, it was observed that the performance of FPSAM is very close to the ideal case where exact channel response at pilot positions is known. To further increase the spectral efficiency, analysis of FPSAM system with multiple antennas at the transmitter and receiver can be taken up as a research issue.

REFERENCES

Cavers, J.K., 1991. An analysis of pilot symbol assisted modulation for Rayleigh fading channels. IEEE T. Veh. Technol., 40(4): 686-693.

Khanna, R. and R. Saxena, 2009. Improved Fractional Fourier Transform Based Receiver for Spatially Multiplexed MIMO Antenna Systems. Wireless Personal Commn., Springer Netherlands, 50(4): 563-574.

Khanna, R. and R. Saxena, 2010. A Novel FRFT Beam former for Rayleigh Faded Channels. Wireless Personal Commn., Springer Netherlands, 52(4): 693-707.

Kutay, M.A., H.M. Ozaktas, O. Arikan and L. Onural, 1997. Optimal filtering in fractional Fourier domains. IEEE T. Signal Proc., 45(5): 1129-1143.

Ozaktas, H.M., B. Barshan, D. Mendlovic and L. Onural, 1994. Convolution, filtering and multiplexing in fractional domains and their relation to chirp and wavelet transforms. J. Optical Soc. America-A, 11(2): 547-559.

Ozaktas, H.M., O. Arikan, M.A. Kutay and G. Bozdagi, 1996. Digital computation of the fractional Fourier transforms. IEEE T. Signal Proc., 44(9): 2141-2150.

Ozaktas, H.M., Z. Zalevsky and M.A. Kutay, 2000. The Fractional Fourier Transform with Applications in Optics and Signal Processing. Wiley, New York.

Proakis, J.G., 2001. Digital Communications. 4th Edn., McGraw-Hill, New York.

Sampei, S. and T. Sunaga, 1993. Rayleigh fading compensation for QAM in land mobile radio communications. IEEE T. Veh. Technol., 42(2): 137-147.

Torrance, J.M. and L. Hanzo, 1995. Comparative study of pilot symbol assisted modem. Radio Receiver and Associated Systems, Conference Publication No. 415, Sep 26-28, pp: 36-41.

Tse, D. and P. Viswanath, 2005. Fundamentals of Wireless Communication. Cambridge University Press, Cambridge.

Webb, W.T. and L. Hanzo, 1994. Modern Quadrature Amplitude Modulation. IEEE Press, New York.

Yetik, I.S., M.A. Kutay, H. Ozaktas and H.M. Ozaktas, 2000. Continuous and discrete fractional Fourier domain decomposition. Proceedings IEEE International Conference Acoustics Speech Signal Processing, pp: 93-96.

Yetik, I.S. and A. Nehorai, 2003. Beamforming using fractional Fourier transform. IEEE T. Signal Proc., 51(6): 1663-1668.